JOURNAL OF CHEMICAL & ENGINEERING DATA

ARTICLE

pubs.acs.org/jced

Adsorption and Selective Separation of Neodymium with Magnetic Alginate Microcapsules Containing the Extractant 2-Ethylhexyl Phosphonic Acid Mono-2-ethylhexyl Ester

Ling Zhang, Dongbei Wu,* Baohui Zhu, Yuhui Yang, and Li Wang

Department of Chemistry, Tongji University, 1239, Siping Road, Shanghai, P. R. China 200092

ABSTRACT: Magnetic alginate microcapsules containing the extractant 2-ethylhexyl phosphonic acid mono-2-ethylhexyl ester (P507) were prepared for adsorption and selective separation of neodymium using equilibrium batch experiments. The effect of various parameters such as adsorbent dose, contact time, temperature, pH, and metal ion concentration on adsorption was investigated. The results demonstrated that the adsorption data fit well the pseudosecond order kinetic model, and the Langmuir adsorption isotherm was suitable for the description of adsorption process. The adsorption capacity had the order $Pb^{2+} > Nd^{3+} > Cu^{2+} > Zn^{2+} > Co^{2+} > Ni^{2+}$ for mono- and multicomponent systems, and Nd^{3+} could be selectively separated from the mixed Nd^{3+}/Co^{2+} and Nd^{3+}/Zn^{2+} solutions over the whole concentration range. Furthermore, solvent extraction and ion exchange mechanisms were confirmed to contribute to the adsorption process by FTIR spectra studies, pH analyses, and adsorption isotherms with possible structures of the complex proposed. Thermogravimetric analysis, desorption, and regeneration tests forecasted that the magnetic alginate P507 microcapsules would be an excellent candidate for their potential industrial application.

INTRODUCTION

Lanthanide elements have gained great attention in the last few decades, owing to their unique properties and wide range of applications, especially in metallurgy, the ceramic industry, and nuclear fuel control.[1] Neodymium, for example, the first triad of the lanthanide series, is representative of all of the most valuable rare earths (REs) that are used in superalloys, electronics components, artistic glasses, optical filters, steel modifiers, and hydrogen storage. Their identical chemical behavior makes difficult the industrial production of high-grade elements.[2]

Currently, solvent extraction is one of the most versatile separation processes with numerous applications in the oil and petrochemical, drug and pharmaceutical, and especially hydrometallurgy industries.[3] The process is well-suited for large-scale continuous operators because of its inherent high capacity and fast kinetics. However, the large amount of organic solution strongly destroys the environment and harms human health, and at the same time, the multistage operations are also laborious and time-wasting. Ion exchange, which is another major hydrometallurgy process, has an advantage over solvent extraction, in that it can be performed in a single-stage operation within a simple packed column.[4] Unfortunately, conventional ion exchanger resins are not as selective as the extractants. Therefore, bridging the gap and combining the merits and drawbacks between solvent extraction and ion exchange became a great stimulus to separation scientists. Among the many proposed techniques, microcapsules containing an extractant is the most popular since it possesses some remarkable advantages such as simplicity of preparation, applicability for a wide range of selective extractants, large special interfacial area, ability for concentration of metal ions from dilute solutions, and less leakage of harmful components to the environment.[5]

Alginate, composed of chains of 1,4-linked β-D-mannuronic acid and α-L-guluronic acid, is the most prominent natural high molecular-weight biopolymer for the preparation of these kinds of microcapsules because of its ease of capsulation, cost efficiency, high acid resistance, and ion-exchange properties for heavy metal ions.[6] Alginate microcapsules have been widely studied for immobilization of living cells, enzymes, and other biologically valuable material.[7] However, few attempts have been done for its separation applications, especially for rare earth ions. Recently, magnetic alginate gel beads and magnetic alginate-chitosan gel beads without any extractant encapsulated were prepared by our research group for adsorption of La(III) ions, and the results demonstrated that alginate had excellent adsorption properties for lanthanum ions.[8,9]

In the present work, magnetic alginate microcapsules containing the extractant 2-ethylhexyl phosphonic acid mono-2-ethylhexyl ester (P507) were prepared. The aim of loading magnetic nanoparticles was to achieve the quick separation of microcapsules from the solution by an external magnet. Little uptake of Nd^{3+} onto pure Fe_3O_4 nanoparticles in a pH 4.0 buffer solution had been verified by the previous work. The extractant 2-ethylhexyl phosphonic acid mono-2-ethylhexyl ester, a kind of acidic organophosphorous extractant, was preferred due to its high separation factor toward rare earth ions.[2] This paper focuses on: (i) studying in detail, the effect of various parameters such as adsorbent dose, temperature, contact time, aqueous pH, and metal ion concentration on the adsorption of neodymium ions; (ii) comparing the adsorption capacity of the Nd^{3+} ion with other metal ions such as Pb^{2+}, Cu^{2+}, Zn^{2+}, Co^{2+}, and Ni^{2+} both in monocomponent systems and in a multicomponent system to discuss the separation selectivity of magnetic alginate P507 microcapsules toward Nd^{3+}

Received: November 27, 2010
Accepted: February 18, 2011
Published: March 10, 2011

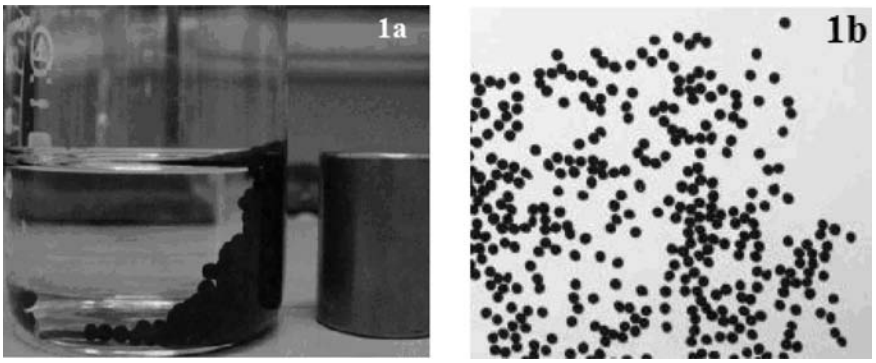

Figure 1. (a) Photograph of magnetic alginate beads attracted by a magnet (S_1). (b) Optical microscopy picture of dry beads (S_1).

ions; and (iii) performing thermogravimetric analysis and desorption and regeneration tests to forecast its potential industrial application.

EXPERIMENTAL SECTION

Chemicals and Reagents. Sodium alginate (Na-alginate), chemical grade from the Shanghai Jingchun Chemical Company of China, was used as received. The extractant 2-ethylhexyl phosphonic acid mono-2-ethylhexyl ester (P507, mass fraction 0.99) was used without further purification. Iron oxide nanoparticles were made by our group using the coprecipitation method reported by Donia.[10] A stock solution of neodymium was prepared from its oxides via dissolution in concentrated hydrochloric acid and standardized by an ethylenediamine tetraacetic acid (EDTA) titration with xylenol orange as the indicator. Other metal ion solutions containing the desired concentrations of Pb^{2+}, Zn^{2+}, Cu^{2+}, Co^{2+}, and Ni^{2+} together were prepared from analytical grade standard solutions (0.5 mol·L^{-1}). The pH was maintained by use of a sodium acetate buffer solution. Ferric chloride hexahydrate, ferrous chloride tetrahydrate, ammonia, calcium chloride dehydrate, and other reagents were analytical grade from China.

Preparation of Microcapsules. The magnetic alginate P507 (2.0 g) microcapsules were prepared according to the methods described elsewhere.[11,12] Briefly, 0.25 g of Fe_3O_4 and 2.0 g of P507 were fully dispersed in the Na-alginate solution (50 cm^3, w = 0.02) with vigorous stirring for 24 h; after that, the magnetic sol was added dropwise into a 0.5 mol·L^{-1} $CaCl_2$ solution through a 1.0 mm (outer diameter) medical needle to cause gellification and form magnetic microcapsules which were gently stirred in the aforementioned solution and incubated for 12 h; finally, they were washed several times with distilled water and dried in a vacuum drying chamber at 55 °C for 24 h. The dried magnetic microcapsules were abbreviated as S_1. Similarly, magnetic alginate P507 microcapsules (S_2) were prepared with 1.0 g of P507. Alginate P507 microcapsules without Fe_3O_4 attached were also prepared by injecting mixed Na-alginate sol and P507 in a $CaCl_2$ solution and were named as S_3. Magnetic alginate beads without P507 (S_4) were prepared by injecting the mixed Na-alginate gel and Fe_3O_4 nanoparticles into a $CaCl_2$ solution. After whole stripping with concentrated HCl, the contents of iron, sodium, and calcium were determined by measuring absorbance using an atomic absorption spectrophotometer (AAS, Perkin-Elmer 3100 model). The P507 content of the beads was checked by measuring the amount of phosphorus by inductively coupled plasma-atomic emission spectroscopy (ICP-AES, Varian Liberty Serie II).[6] The amounts of the different species are expressed in millimoles per gram of dried beads. Figure 1a shows that the magnetic alginate P507 microcapsules could be easily removed by an external magnet.

Batch Studies. All equilibrium adsorption experiments were conducted for Nd^{3+}, Pb^{2+}, Zn^{2+}, Cu^{2+}, Co^{2+}, and Ni^{2+} in a thermostatted shaker maintained at 298 K for 20 h by shaking 50 mg of the gel beads in 50 mL of metal solution taking varying concentrations in the range of 0.1 mmol·L^{-1} to 3.0 mmol·L^{-1} at pH 4.0. After attaining equilibrium, the sorbent was separated by an external magnet. The adsorption capacity of the sorbent was determined by material balance of the initial and equilibrium concentration of the solution. The adsorption parameters such as adsorbed amount (q_e), distribution ratio (D), separation factor (S), and uptake efficiency (%) are defined by the following equations

$$q_e = (C_{ini} - C_e)V/m \quad (1)$$

$$D = q_e/(q_{ini} - q_e) \quad (2)$$

$$S = D_1/D_2 \quad (3)$$

$$\text{Uptake } (\%) = q_e/q_{ini} \cdot 100 \quad (4)$$

where $q_e/(mg \cdot g^{-1})$ and $q_{ini}/(mg \cdot g^{-1})$ are the uptake and initial neodymium concentrations, respectively. $C_e/(mg \cdot L^{-1})$ and $C_{ini}/(mg \cdot L^{-1})$ denote the equilibrium and initial aqueous concentrations of Nd^{3+} ions. V/mL is the total volume of the solution in liters, and m/g^{-1} is the mass of the dry magnetic beads used in grams. D_1 and D_2 are the distribution ratio of the first metal (Nd^{3+}) and the second metal ion (Zn^{2+}, Co^{2+}, or Ni^{2+}), respectively.

The adsorption isotherms for monocomponent and multicomponent systems were analyzed with the Langmuir (eq 5) and Freundlich (eq 6), respectively.

$$\frac{C_e}{q_e} = \frac{C_e}{q_{max}} + \frac{1}{bq_{max}} \quad (5)$$

$$\log q_e = \log K_F + \frac{1}{n} \log C_e \quad (6)$$

where $q_{max}/(mg \cdot g^{-1})$ is the maximum adsorption capacity; $b/(L \cdot mg^{-1})$ is the Langmuir parameter; $K_F/((mg \cdot g^{-1})(L \cdot g^{-1})^n)$ is the Freundlich constant suggesting adsorption capacity; and $1/n$ is the Freundlich constant indicating adsorption intensity.

For the monocomponent system, the concentration of neodymium in the supernatant was determined by measuring absorbance

Table 1. Bead Characteristics[a]

	S_1	S_2	S_3	S_4
average weight of each dried bead (mg)	0.64	0.58	0.53	0.50
diameter/(mm)	0.83 ± 0.04	0.82 ± 0.03	0.80 ± 0.04	0.92 ± 0.03
[Na]/(mmol·g^{-1})	0.28	0.36	-	-
[Fe]/(mmol·g^{-1})	0.92	1.35	-	-
[Ca]/(mmol·g^{-1})	2.82	3.04	-	-
estimation of P507 using ICP-AES	1.86	1.33	-	-

[a] The amounts of iron, calcium, and P507 are expressed in mmol·g^{-1} of dried beads.

using a UV−vis spectrophotometer (China, model UV-752) with arsenazo-III as a chromomeric reagent. The residual concentrations of other metal ions such as Pb^{2+}, Zn^{2+}, Cu^{2+}, Co^{2+}, and Ni^{2+} were volumetrically analyzed with EDTA methods. For the multicomponent systems, the initial salt solution mixture, containing equivalent Pb^{2+}, Nd^{3+}, Zn^{2+}, Cu^{2+}, Co^{2+}, and Ni^{2+} (from 0.1 mmol·L^{-1} to 3.0 mmol·L^{-1}) concentrations was prepared in a standard acetate buffer solution at pH 4.0, and the residual concentrations of metal ions were determined by ICP-AES. The determinations were repeated three times with the standard deviation within 5 %.

Similar to the above procedure, the effect of adsorption dose on the adsorption was performed at the conditions: pH 4.0, contact time of 20 h, and temperature of 298 K with initial neodymium concentration of 0.5 mmol·L^{-1}. The effect of time on the adsorption was done at a pH of 4.0, temperature of 298 K, and the initial metal ion concentrations of 0.5 mmol·L^{-1} and 1.0 mmol·L^{-1} with the adsorbent dose of 0.05 g. The effect of pH on the adsorption was studied at a temperature of 298 K, initial metal ion concentration of 0.5 mmol·L^{-1}, and contact time of 20 h with the adsorbent dose of 0.05 g.

FTIR Spectral and Thermal Analyses. Fourier transform infrared spectra of P507, magnetic alginate P507 microcapsules before and after adsorption of neodymium ions, were recorded over the frequency range from (4000 to 500) cm^{-1} using a FTIR spectrophotometer (USA, model Nicolet Avatar 360). The samples were formed into pellets with KBr. A thermal analyzer (model Netzch TG 209) was used in the temperature range of (10 to 800) °C at a heating rate of 10 °C·min^{-1} with nitrogen flushed at 200 mL·min^{-1}.

Desorption and Regeneration Studies. To evaluate the reusability of the sorbent, adsorption of Nd^{3+} and regeneration of Nd-loaded magnetic alginate P507 microcapsules were performed in three consecutive adsorption−desorption cycles. In each cycle, 0.5 mmol·L^{-1} Nd^{3+} in 50 mL of solution was mixed with 50 mg of dried magnetic beads for 20 h. The magnetic microcapsules were separated magnetically, and the supernatant composed of neodymium, calcium, and iron was subjected to measurements. The resultant Nd-loaded sorbent was mixed with 50 mL of 0.1 mol·L^{-1} HCl solution for 20 h. Prior to the next adsorption−desorption cycle, regenerated magnetic microcapsules were washed thoroughly with distilled water until pH 6.2.

RESULTS AND DISCUSSION

Characterization of the Adsorbent. The microcapsules were observed with an optical microscope (Leica) equipped with a digital image camera and video monitor. Digital photographs of the microcapsules were used in combination with image analysis software (Image J) to obtain their mean diameter and size distribution. To verify the reproducibility of the microcapsule preparation, three different samples of 100 microcapsules were analyzed for each preparation. Figure 1b gives a picture of the S_1 dried microcapsules, and the results obtained for different synthesis showed good reproducibility. Table 1 reports the principal characteristics of S_1 and S_2 such as their weight, mean diameter, calcium ion, sodium ion, iron ion, and P507 contents. The iron contents of the beads (0.92 mmol·g^{-1} for S_1 and 1.35 mmol·g^{-1} for S_2) were close to the amounts of magnetic nanoparticles initially added to the alginate solution (1.0 mmol·g^{-1} for S_1 and 1.40 mmol·g^{-1} for S_2). The sodium amounts were weak compared to calcium due to the ionic exchange between these two ions at the time of the gelation process. For P507, their contents in the beads (1.86 mmol·g^{-1} for S_1 and 1.33 mmol·g^{-1} for S_2) were less than the amounts of P507 initially added to the alginate solution (2.0 mmol·g^{-1} for S_1 and 1.45 mmol·g^{-1} for S_2), which originated from the leakage of P507 in the process of vacuum drying.

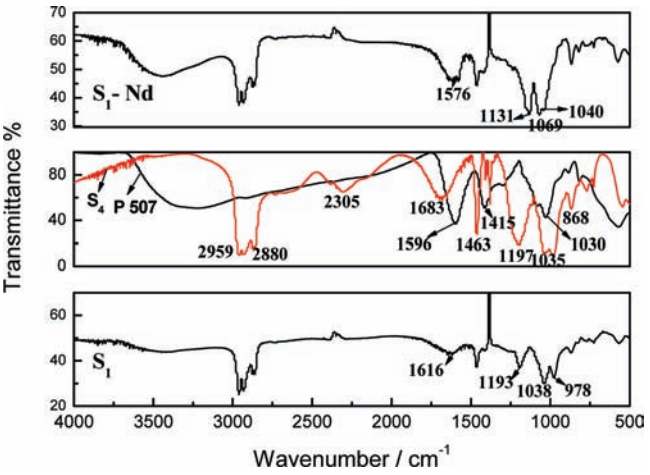

Figure 2. FT-IR spectra of P507, S_1, and S_1−Nd. The initial concentration of Nd^{3+} is 0.5 mmol·L^{-1}.

FT-IR analysis was performed to characterize pure P507, magnetic alginate microsphere (S_4), and the magnetic alginate P507 microcapsules (S_1) (Figure 2). The characteristic peaks of P507 such as P(O)OH, dimeric P═O, and P−OH stretching vibrations are indexed in Table 2.[12] The characteristic peaks of S_4 such as −COOH at around 1600 cm^{-1} were reported in our earlier work.[8] Comparing pure P507 with S_1, it can be observed that the characteristic peaks of P507 had no obvious changes, suggesting that P507 was fully encapsulated into the alginate gel beads. The peak at 1610 cm^{-1} was assigned to be the −COOH stretching vibration in the alginate.[13] Comparing the FT-IR spectra of the magnetic alginate 507 beads (S_1) before and after adsorption of Nd^{3+} (S_1−Nd), a significant change in the FTIR

Table 2. Characteristic Peak of the P507 IR Spectrum

$\nu/(cm^{-1})$	
2959, 2930, 2880	C−H stretching
2305, 1683	P(O)OH vibrations characteristic of the phosphinic group
1463, 1407	confirm the presence of more than one CH_3 group on a carbon atom
1198	dimer form of P═O stretching
1037	P−OH stretching
984	P−O−C stretching
868	P−C stretching

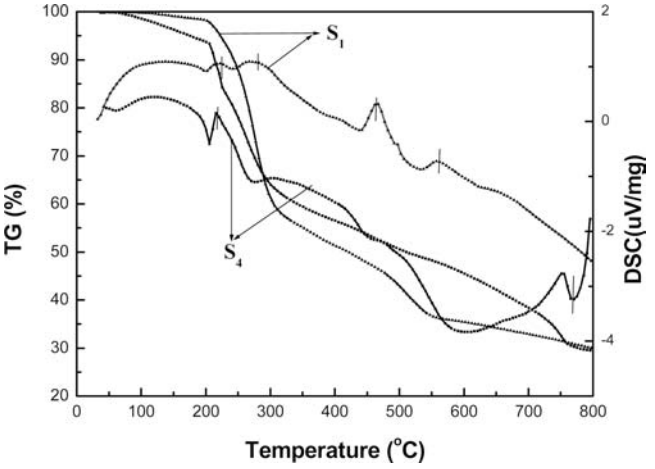

Figure 3. TG and DSC curves for magnetic alginate beads and magnetic alginate P507 microcapsules.

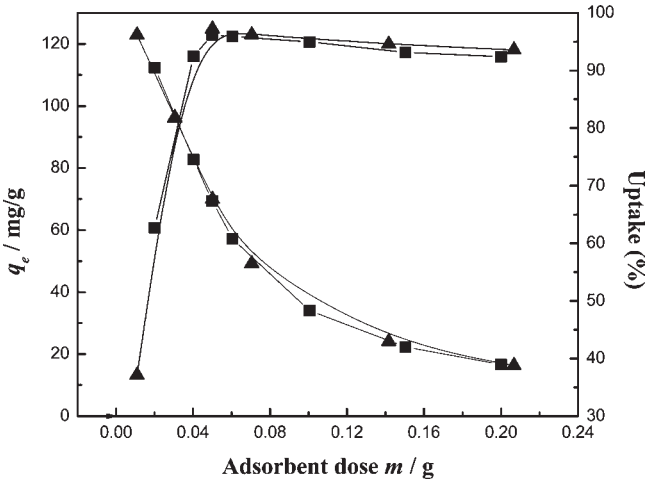

Figure 4. Effect of adsorbent dose on adsorption. T = 298 K, pH = 4.0, equilibrium time = 20 h. ▲, S_1; ■, S_2.

spectra was found for the absorption band at 1193 cm^{-1}, corresponding to the dimeric form of the P═O stretching vibration, which became sharper and shifted to a lower wavenumber. The peaks at 1038 cm^{-1} which were assigned to the P−OH stretching vibration and 978 cm^{-1} corresponding to the P−O−C stretching vibration, respectively, became sharper and shifted to higher wavenumbers, suggesting that the extraction mechanism contributed to the adsorption. Another major change in the FTIR spectra was observed at the absorption bands of 1616 cm^{-1}, assigned to the stretching vibration of −COOH in the alginate, which became stronger and shifted to a lower wavenumber after Nd^{3+} adsorption. The result revealed that the carboxyl groups of the alginate participated in the adsorption process.

The thermal stabilities of magnetic alginate beads (S_4) and magnetic alginate P507 beads (S_1) were investigated and compared. The result from thermogravimetric analysis is shown in Figure 3. The curves of TG indicated three weight loss ranges: from (0 to 200) °C, (200 to 300) °C, and (300 to 800) °C. The first weight loss was considered to be due to the evaporation of water. The second significant weight loss for S_4 was a mass fraction of 0.35 with a sharp endothermic peak at 210 °C, which could be attributed to the desorption and degradation of alginate,[8] while in the case of S_1, two small endothermic peaks appeared at (210 and 270) °C. The former is due to desorption and degradation of alginate, and the latter maybe arose from the reaction between the degraded alginate and P507. The third distinct weight loss for S_1 could be attributed to further decomposition of alginate and gasification of degradation products. For S_1, the presence of two endothermic peaks at (460 and 510) °C was a signal that a kind of chemical reaction or further degradation between the first degradation product of alginate and P507 takes place at temperatures more than 400 °C. In short, from the TG and DSC analyses of the biosorbents, it was concluded that S_1 could be used even at high temperatures.[14]

Effect of Adsorbent Dose. The adsorbent dose is an important influential factor for adsorption equilibrium. To select the most suitable adsorbent dose, the dependence of the adsorbent (S_1, S_2) dosage on Nd^{3+} adsorption was studied, and the results are shown in Figure 4. In this experiment, the amount of adsorbents used was varied from (0.02 to 0.2) g while keeping the other parameters such as pH, metal solution volume, concentration, and contact time constant. It was found that the adsorption capacity of the metal ion per unit mass of biosorbent ($mg \cdot g^{-1}$) decreased with the increase in dose of adsorbent, which was attributed to lower utilization of adsorption capacity of the sorbent at higher dosage.[15] On the contrary, the uptake percentage increased with increasing adsorbent doses when the adsorbent dose was less than 0.05 g. This was expected since the number of adsorption sites available for adsorbent−adsorbate interaction increased with increasing adsorbent doses. Moreover, it showed that the uptake efficiency decreased slightly when the adsorbent dose was more than 0.05 g, which might be due to a blocking of the porous channel in the microcapsule.[16] Therefore, the optimum adsorbent dose for extraction was defined to be 0.05 g.

Adsorption Kinetics. The effect of contact time on the adsorption equilibrium at different initial metal ion concentrations is shown in Figure 5a. The adsorption efficiency increased with time and attained an equilibrium within 5 h for S_1, 8 h for S_2,

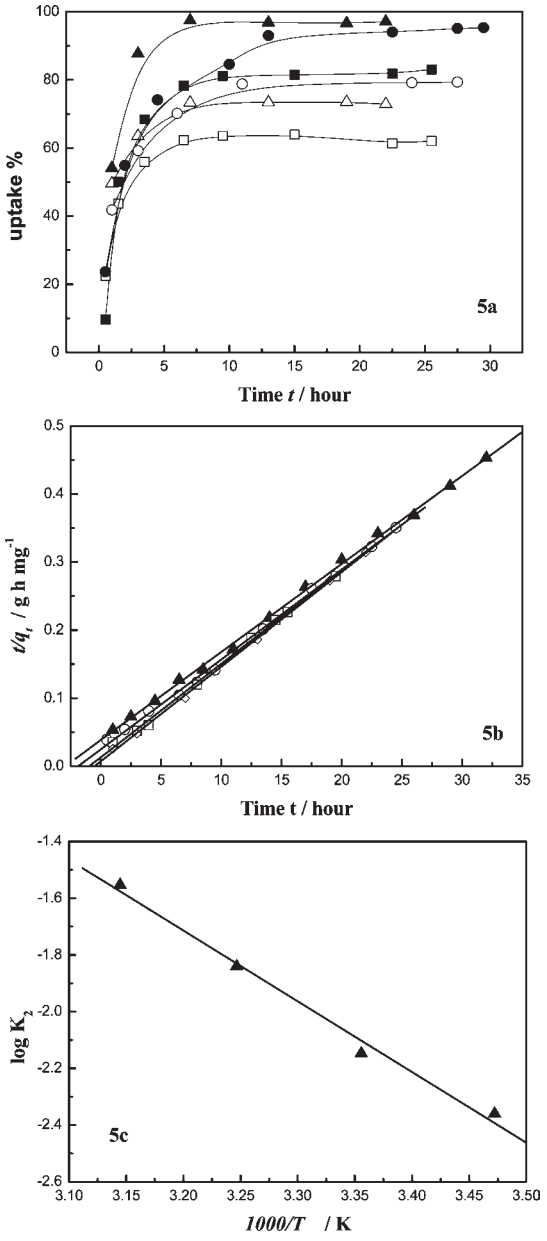

Figure 5. (a) Adsorption kinetics of S_1, S_2, and S_3. T = 298 K, pH = 4.0, m = 0.05 g, ▲, S_1, $C_{ini}(Nd^{3+})$ = 0.5 mmol·L^{-1}; Δ, S_1, $C_{ini}(Nd^{3+})$ = 1.0 mmol·L^{-1}; ■, S_2, $C_{ini}(Nd^{3+})$ = 0.5 mmol·L^{-1}; □, S_2, $C_{ini}(Nd^{3+})$ = 1.0 mmol·L^{-1}; ●, S_3, $C_{ini}(Nd^{3+})$ = 0.5 mmol·L^{-1}; ○, S_3, $C_{ini}(Nd^{3+})$ = 1.0 mmol·L^{-1}. (b) Pseudosecond-order plots for the adsorption of Nd^{3+} on the S_1 gel bead at various temperatures. $C_{ini}(Nd^{3+})$ = 0.5 mmol·L^{-1}, m = 0.05 g, T = 298 K, pH = 4.0. ○, T = 288 K; ▲, T = 298 K; □, T = 308 K; ◇, T = 318 K. (c) Corresponding Arrhenius plot of S_1 gel bead at various temperatures. $C_{ini}(Nd^{3+})$ = 0.5 mmol·L^{-1}, m = 0.05 g, pH = 4.0.

and 11 h for S_3, respectively. After the equilibrium period, the adsorbed amount of metal ions did not change significantly with time. A greater initial metal ion concentration would result in a higher adsorption capacity. This can be due to a higher probability of collision between metal ions and the adsorbent surface and a better driving force, which lessens the mass transfer resistance.[17]

To investigate the adsorption mechanism, the observed data were analyzed in terms of various kinetic models, among which the pseudosecond order rate law was the best fit. The linear equation

Table 3. Data of Adsorption Kinetics

adsorbent	concentration of metal ions (mmol·L^{-1})	K_2 (100·g/mg·h)	R^2	q_e (mg·g^{-1})
S_1	0.5	2.80	0.9990	76.9
	1.0	2.70	0.9991	111.1
S_2	0.5	1.97	0.9990	62.5
	1.0	2.01	0.9984	100.1
S_3	0.5	1.15	0.9990	71.4
	1.0	0.80	0.9991	125.0

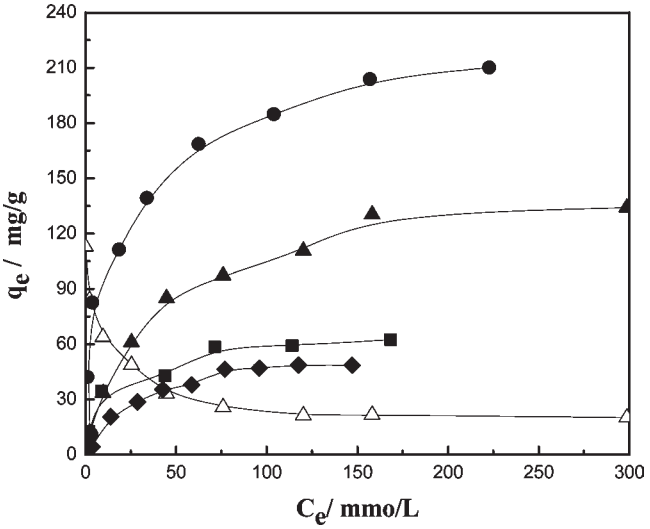

Figure 6. Adsorption isotherms of Nd^{3+} using S_1, S_2, S_3, and S_4 as adsorbents in the monocomponent solutions. m = 0.05 g, T = 298 K, pH = 4.0, equilibrium time = 20 h. ▲, S_1—Nd; ■, S_2—Nd; ●, S_3—Nd; ♦, S_4—Nd; Δ, S_1—Ca.

of the pseudosecond order reaction is given as eq 7

$$\frac{t}{q_t} = \frac{1}{k_2 q_e^2} + \frac{t}{q_e} \quad (7)$$

The variables q_t and q_e represent the adsorption capacity (mg·g^{-1}) at time t (h) and equilibrium, respectively. The pseudosecond order constant k_2 (g·mg^{-1}·h^{-1}) could be determined experimentally from the intercept of plot t/q_t versus t. Table 3 gives the values of the pseudosecond order reaction parameters for S_1, S_2, and S_3, respectively. Comparing the values of k_2 (S_1) with those of k_2 (S_3), it can be calculated that the adsorption rate was increased by up to 2.3 to 3.4 times, clearly indicating that the adsorption rate was greatly enhanced by a combination of Fe_3O_4 with alginate. A reasonable explanation is that the attachment of Fe_3O_4 may lead to an increase of the ratio surface and the internal diameter of the microcapsule.[18] Meanwhile, the skeleton of alginate is well preserved in the process of vacuum drying due to the doping of Fe_3O_4 nanoparticles. While comparing S_1 with S_2, it can be observed that the adsorption capacity increased as the mass of P507 increased, suggesting that P507 would exert a positive influence on the adsorption.

A plot of t/q_t as a function of time t is illustrated in Figure 5b. The points lie on straight lines corresponding to each temperature as expected from eq 7. From the relationship between the

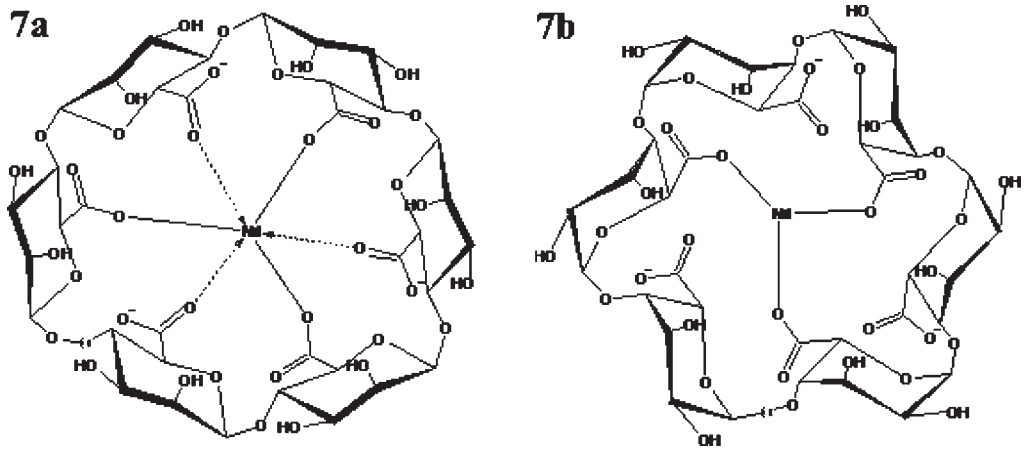

Figure 7. Complex structures of alginate with Nd^{3+}. (a) β-D-Mannose (M−M)−Nd^{3+} and (b) α-L-golose (G−G)−Nd^{3+}.

evaluated rate constant and temperature, an Arrhenius plot was obtained according to eq 8 as shown in Figure 5c, from which the apparent activation energy, E_a, was evaluated to be (20.75 ± 0.08) kJ·mol^{-1} with R^2 equal to 0.99. Because physical adsorption is usually weak, the energy requirement is also small, and such values are less than 5 kJ·mol^{-1}. Chemical adsorption is stronger and needs higher activation energy.[19] These facts suggest that the adsorption of Nd^{3+} onto the magnetic alginate P507 beads was a chemical phenomenon and also an endothermic process.

$$\ln K = -\frac{E_a}{RT} + B \qquad (8)$$

Adsorption Isotherm and Ion Exchange Mechanism. Adsorption isotherms of Nd^{3+} in the monocomponent solutions with S_1, S_2, S_3, and S_4 are shown in Figure 6. The adsorption capacity of the adsorbents (S_1, S_2, S_3, and S_4) increased with increasing equilibrium concentrations of metal ion and then reached a constant value in the higher equilibrium concentration range. The order of adsorption capacity of S_1, S_2, S_3, and S_4 was $S_3 > S_1 > S_2 > S_4$, indicating that P507 could improve the adsorption efficiency. On the basis of eq 5, the maximum adsorption capacities evaluated by the Langmuir equation for S_1, S_2, S_3, and S_4 were (149.3 ± 0.05) mg·g^{-1} (1.03 mmol·g^{-1}), (64.1 ± 0.07) mg·g^{-1} (0.44 mmol·g^{-1}), (217.4 ± 0.03) mg·g^{-1} (1.51 mmol·g^{-1}), and (51.3 ± 0.03) mg·g^{-1} (0.37 mmol·g^{-1}), respectively. The constants b for S_1, S_2, S_3, and S_4 were 0.034 L·mg^{-1}, 0.007 L·mg^{-1}, 0.008 L·mg^{-1}, and 0.003 L·mg^{-1}, respectively. The experimental data concluded that the adsorption process was fit well by the Langmuir isotherm model ($R^2 > 0.99$). By considering a complex of one Nd^{3+} with three P507 molecules, for S_1, the expected neodymium uptake should be about 0.62 mmol·g^{-1}, and the amount of exchangeable neodymium with calcium ions of alginate was equal to 0.41 mmol·g^{-1}, which approached the values obtained by S_4; while in the case of S_2, the expected neodymium uptake should be about 0.44 mmol·g^{-1}, and the amount of exchangeable neodymium with calcium ions of alginate was almost zero, indicating a weaker affinity of alginate than that of P507 toward Nd^{3+} which was consistent with the conclusion reported by Mohammad et al.[6] Furthermore, Figure 6 shows that calcium ions were released from S_1 as neodymium ions were gradually adsorbed by them. The uptake of neodymium was thus governed by an ion exchange reaction. This phenomenon, when the amount of released calcium ions was equal to 0.53 mmol·g^{-1} the amount of adsorbed neodymium reached 0.93

Table 4. Calculated Langmuir and Freundlich Isotherm Constant Values[a]

	R_L	
C_{ini}/(mmol·L^{-1})	S_1	S_2
0.3	0.40	0.76
0.6	0.25	0.62
0.9	0.18	0.52
1.2	0.14	0.45
1.6	0.11	0.38
2.0	0.09	0.33
3.0	0.06	0.24

(a)

model	parameters	Pb^{2+}	Nd^{3+}	Cu^{2+}	Zn^{2+}	Co^{2+}	Ni^{2+}
Langmuir	q_m/(mg·g^{-1})	-	149.3	-	61.73	-	-
	b/(L·mg^{-1})	-	34.0	-	416	-	-
	R^2	-	0.9952	-	0.9993	-	-
Freundlich	K_f/(mg·g^{-1})(L·g^{-1})^n	10.9	-	0.64	-	0.65	0.20
	$1/n$	0.53	-	1.83	-	0.75	0.83
	R^2	0.9882	-	0.9525	-	0.9607	0.9611

(b)

model	parameters	Pb^{2+}	Nd^{3+}	Cu^{2+}	Zn^{2+}	Co^{2+}	Ni^{2+}
Langmuir	q_m/(mg·g^{-1})	-	45.5	-	12.0	-	-
	b/(L·mg^{-1})	-	4.23	-	4.61	-	-
	R^2	-	0.9866	-	0.9854	-	-
Freundlich	K_f/(mg·g^{-1})(L·g^{-1})^n	5.10	-	1.46	-	0.21	-
	$1/n$	0.49	-	0.95	-	0.68	-
	R^2	0.9825	-	0.9993	-	0.9572	-

(c)

[a] (a) The values of R_L at the different initial concentrations of Nd^{3+}. (b) Langmuir and Freundlich isotherm constants for Pb^{2+}, Nd^{3+}, Cu^{2+}, Zn^{2+}, Co^{2+}, and Ni^{2+} on S_1 for monocomponent systems. (c) Langmuir and Freundlich isotherm constants for Pb^{2+}, Nd^{3+}, Cu^{2+}, Zn^{2+}, Co^{2+}, and Ni^{2+} on S_1 for multicomponent systems.

dx.doi.org/10.1021/je101270j |J. Chem. Eng. Data 2011, 56, 2280–2289

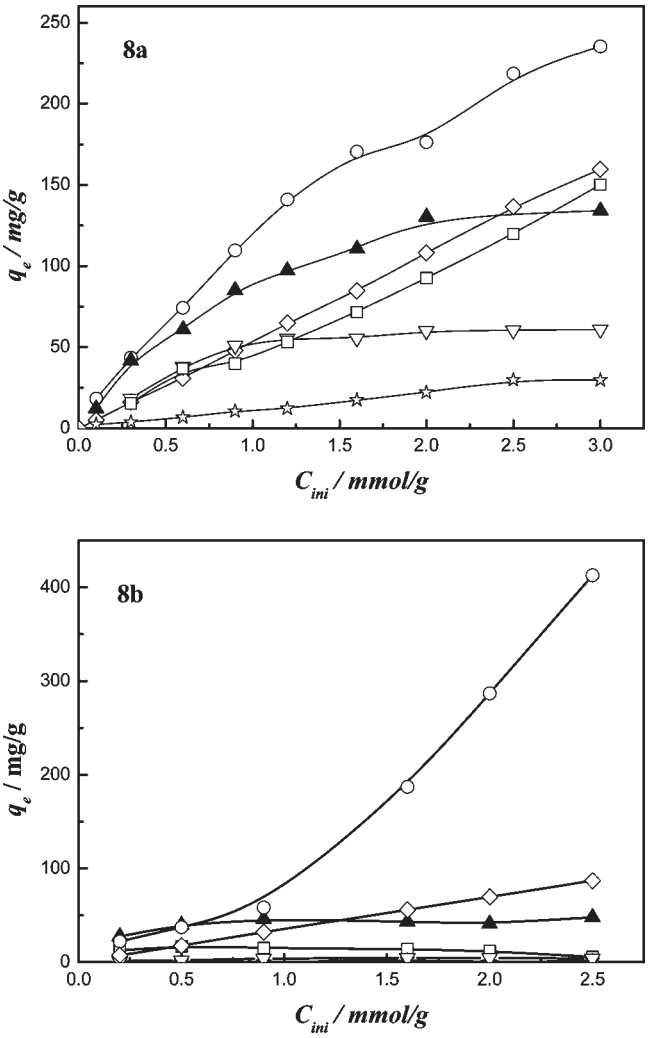

Figure 8. Effect of initial concentration on the adsorption. (a) For the monocomponent solution (S_1). (b) For the multicomponent solution (S_1). m = 0.05 g, T = 298 K, pH = 4.0, equilibrium time = 20 h. ▲, Nd^{3+}; ○, Pb^{2+}; ◇, Cu^{2+}; □, Zn^{2+}; ▽, Co^{2+}; ☆, Ni^{2+}.

Table 5. Electronic Configurations and Hydra Ion Radii of Different Metal Ions

metal ion	Pb^{2+}	Nd^{3+}	Cu^{2+}	Zn^{2+}	Co^{2+}	Ni^{2+}
electronic configuration	$6s^2$	$4f^4 5s^2 5p^6 5d^9$	$3d^9$	$3d^{10}$	$3d^7$	$3d^8$
block	p	f	ds	ds	d	d
hydra ion radium	1.2	1.0	0.72	0.74	0.74	0.72

$mmol \cdot g^{-1}$ (0.62 $mmol \cdot g^{-1}$ with P507 and 0.31 $mmol \cdot g^{-1}$ with calcium alginate), might be a symbol that three Ca^{2+} were replaced by two Nd^{3+} at pH 4.0. The ion exchange between alginate and Nd^{3+} can thus be written as eq 9

$$2Nd^{3+} + 3Ca(A\,lg)_2 = 2Nd(A\,lg)_3 + 3Ca^{2+} \qquad (9)$$

A possible complex structure between alginate and Nd^{3+} is shown in Figure 7. As is well-known, alginate is a natural linear polysaccharide composed of β-D-mannuronate acid (M) and α-L-guluronate acid (G), linked by β-1,4- and α-1,4-glycosidic bonds. M and G units are organized in homopolymer M−M and G−G blocks

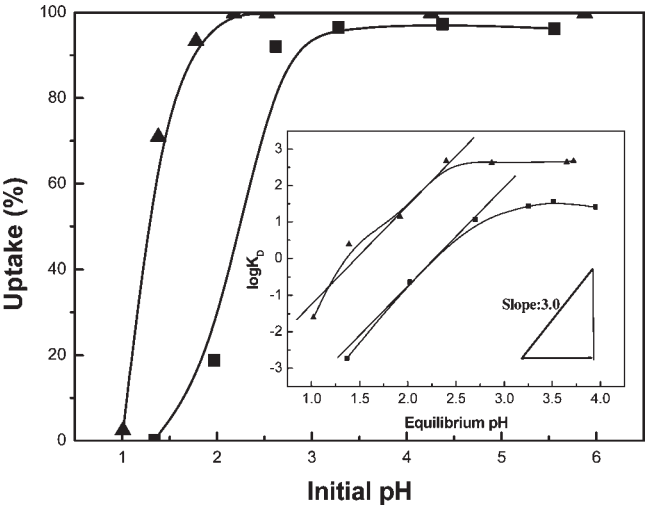

Figure 9. Effect of pH on adsorption. C_{ini} = 0.5 $mmol \cdot L^{-1}$, T = 298 K, m = 0.05 g, equilibrium time = 20 h. ▲, S_1; ■, S_2.

and heteropolymeric M−G blocks. The proportions of these blocks vary with the source of the alginate polymer and are difficult to indentify, thus the formation of a complex between M−G with Nd^{3+} has not been provided. Furthermore, it has been verified that alginate is attached to iron oxide via the interaction between the carboxylic groups of alginate and the surface hydroxyl groups of iron oxide,[16] and the −O− of the carboxylic groups in Figure 7 thus could be supposed to be bound with free Ca^{2+} and Fe_3O_4 nanoparticles, which was positively charged due to the formation of $Fe(OH_2)^+$ at lower pH.

A further analysis of the Langmuir equation can be made on the basis of a dimensionless equilibrium parameter, R_L, also known as

$$R_L = \frac{1}{1 + bC_{ini}} \qquad (10)$$

where C_{ini} is the initial concentration of Nd^{3+} expressed in milligrams per liter and b is the Langmuir adsorption equilibrium constant ($L \cdot mg^{-1}$). If the value of R_L was equal to zero or one, the adsorption is either linear or irreversible, and if the value is in between zero and one, adsorption was favorable to chemisorption.[11] As shown in Table 4a, the values of R_L at 298 K lie between 0.06 to 0.40 for S_1 and 0.24 to 0.76 for S_2 indicating the suitability of S_1 and S_2 for the uptake of Nd^{3+}. Moreover, to our knowledge, only the research group of Su has reported Nd^{3+} adsorption with neodymium ion imprinted polymer particles (Nd^{3+}-IIP), which were prepared by the copolymerization of Nd^{3+}-5,7-dichloroquinoline-8-ol-4-vinylpyridine ternary complexes with styrene and divinyl benzene,[20] and little other information has been reported on the adsorption of neodymium; therefore, it is difficult to compare the adsorption characteristics of magnetic alginate P507 microcapsules with other adsorbents. According to the result obtained from Su, i.e., the adsorption capacity of the Nd^{3+}-IIP was 35.18 $mg \cdot g^{-1}$, the adsorption capacity value reported in the present study was therefore comparable to the above value.

The effects of initial concentration of other metal ions such as Pb^{2+}, Zn^{2+}, Cu^{2+}, Co^{2+}, and Ni^{2+} on the adsorption in the monocomponent and multicomponent solution were also performed in the same conditions, and the results are illustrated in Figure 8a and Figure 8b. The magnetic alginate P507 beads

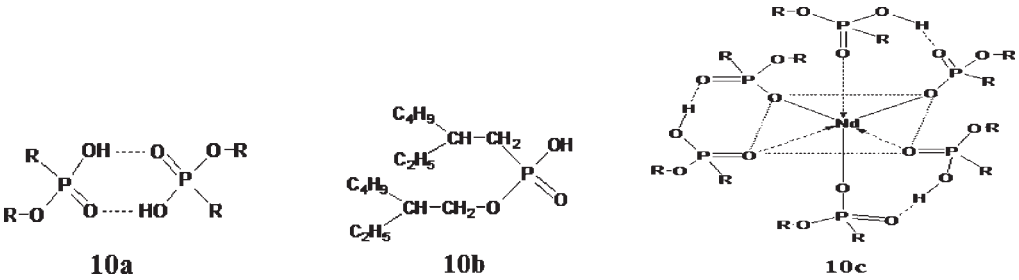

Figure 10. Structures of P507, P507 dimer, and its complexes with Nd^{3+}. (a) P507; (b) form of dimer $(HL)_2$ associated by the hydrogen bonds between their two molecules; and (c) P507−Nd bonds for extraction.

Table 6. Selective Separation of Nd^{3+} from the Mixed Nd^{3+}/Zn^{2+}, Nd^{3+}/Co^{2+}, and Nd^{3+}/Ni^{2+} Solutions at Various Initial Metal Ion Concentrations

	Nd^{3+}/Zn^{2+}			Nd^{3+}/Co^{2+}			Nd^{3+}/Ni^{2+}		
C_{ini}	q_e(Nd)	q_e(Zn)		q_e(Nd)	q_e(Co)		q_e(Nd)	q_e(Ni)	
($mmol \cdot L^{-1}$)	($mg \cdot g^{-1}$)	($mg \cdot g^{-1}$)	$S_{(Nd/Zn)}$	($mg \cdot g^{-1}$)	($mg \cdot g^{-1}$)	$S_{(Nd/Co)}$	($mg \cdot g^{-1}$)	($mg \cdot g^{-1}$)	$S_{(Nd/Ni)}$
0.5	62.9	23.2	2.75	65.6	3.36	78.3	67.5	0.145	1377
1.0	87.5	22.1	3.00	97.6	3.43	33.8	107.6	0.69	129.8
1.5	112	23.8	3.35	132.4	7.89	16.0	140.4	0.015	6342
2.0	126	24.6	3.34	154.4	11.0	11.1	162.4	0.28	326.2
2.5	154	21.8	4.87	170.9	11.7	10.4	192.0	0.225	490.5

Table 7. Regeneration of Beads by Consecutive Uptake/Desorption Cycles[a]

	first recycle	second recycle	third recycle
uptake/(%)	97.1	91.5	86.7
desorption/(%)	90.2	88.4	85.6
$Ca_{[released]}$/(%)	3.23	5.42	6.80
$Fe_{[released]}$ (%)	5.41	7.83	8.92

[a] Adsorption is realized at pH 4.0. Desorption occurs by elution with hydrochloric acid at pH 1.0. $C_{ini}(Nd^{3+}) = 0.5$ mmol·L^{-1}, $m = 0.05$ g of dry magnetic bead, $V = 50$ mL, $T = 298$ K.

demonstrated excellent adsorption abilities for all the metal ions in the monocomponent systems. While in the case of the multicomponent system, the absorbed amount of Pb^{2+} was higher than that in the monocomponent system, and the adsorbed amount of the other metal ions was less than that in the monocomponent system, especially for Ni^{2+} as its concentration in the supernatant almost could not be determined in the multicomponent system. This was expected since there was ion competition for the adsorbent active sites.[21] The adsorption efficiency had the following order, $Pb^{2+} > Nd^{2+} > Cu^{2+} > Zn^{2+} > Co^{2+} > Ni^{2+}$, which might arise from different adsorption mechanisms. As seen in Table 4b and Table 4c, the adsorptions of Nd^{3+} and Zn^{2+} followed the Langmuir models no matter whether they were in a monocomponent system or in a multicomponent system, indicating that the adsorption was monolayer adsorption on a homogeneous surface. While in the case of Pb^{2+}, Co^{2+}, Cu^{2+}, and Ni^{2+}, their adsorptions can be explained by the Freundlich isotherm models, suggesting non-ideal adsorption on heterogeneous surfaces. Furthermore, the different affinities between the metal and the functional groups on the sorbent also caused the variation in metal removal efficiency.[22] Finally, different electronic configurations and hydrated ion radii may contribute to the different adsorption capacity (Table 5). Jeon et al. reported heavy metal ion adsorptions with magnetic modified alginic acid as a sorbent, and the results demonstrated that the selectivity for metals was Pb ≫ Cu > Cd > Zn > Co > Ni.[23]

pH Effect and Solvent Extraction Mechanism. The effect of pH on adsorption was studied in Figure 9, and the Nd^{3+} ion uptake increased as pH increased from 1.0 to 2.0 for S_1 and 1.0 to 3.0 for S_2. The maximum uptake of Nd^{3+} ions took place above pH 2.0 for S_1 and pH 3.0 for S_2, exhibiting that the adsorption efficiency increased as the content of P507 increased, and this result was consistent with the above results obtained from the adsorption isotherm. At pH 1.0, the removal efficiency was very low, demonstrating that the adsorbents could be eluted commendably with a 0.1 mol·L^{-1} acidic solution. Above pH 3.0, the uptake efficiency of S_1 and S_2 was nearly 100 % and 98 %, respectively. By determining the values of final pH, it could be observed that the values of final pH were less than that of initial pH values, indicating a release of hydrogen ions. Plotting the logarithmic distribution coefficient of Nd^{3+} against equilibrium pH, a linear equation with a slope of 3.0 could be obtained, which was an indicator that the uptake of Nd^{3+} precedes by the following extraction reaction

$$Nd^{3+} + 3H_2L_{2(O)} \rightarrow NdL_3(HL)_{3(O)} + 3H^+ \qquad (11)$$

where HL denotes the P507; $(HL)_2$ is the dimeric form of P507; and the subscript (O) refers to the organic phase. According to Park et al.,[24] P507 and its extracted complexes can be drawn as Figure 10.

dx.doi.org/10.1021/je101270j |J. Chem. Eng. Data 2011, 56, 2280–2289

Selective Separation of Nd^{3+} from the Mixed Nd^{3+}/Zn^{2+}, Nd^{3+}/Co^{2+}, and Nd^{3+}/Ni^{2+} Systems at Various Initial Metal Ion Concentrations. The selective separation was achieved by mixing Nd^{3+} with equal amount of Zn^{2+}, Co^{2+}, or Ni^{2+} in the concentration range from 0.5 mmol·L^{-1} to 2.5 mmol·L^{-1} at the pH of 4.0, temperature of 298 K, and contact time of 20 h with the adsorbent dose of 0.05 g. Table 6 shows the selective separation of Nd^{3+} from the mixed Nd^{3+}/Zn^{2+}, Nd^{3+}/Co^{2+}, and Nd^{3+}/Ni^{2+} solutions at various initial metal ion concentrations. The results demonstrated that the separation of Nd^{3+} from mixed Nd^{3+}/Zn^{2+} solution was possible, especially at higher metal ion concentrations such as the 2.5 mmol·L^{-1} Nd^{3+} + 2.5 mmol·L^{-1} Zn^{2+} system where the value of the separation coefficient of $S_{(Nd/Zn)}$ reached 4.89 with the adsorbed amount of Nd^{3+} of 154 mg·g^{-1} contrasting to that of Zn^{2+} of 21.8 mg·g^{-1}. In the case of the mixed Nd^{3+}/Co^{2+} and Nd^{3+}/Ni^{2+} systems, with so large separation coefficients, for example, the values of $S_{Nd/Co}$ ranged from 10.4 to 78.3, and that of $S_{Nd/Ni}$ increased from 129 to 6342 clearly indicating that it would be easy to separate Nd^{3+} from the mixed Nd^{3+}/Co^{2+} and Nd^{3+}/Ni^{2+} solutions over the whole metal ion concentration range.

Desorption and Regeneration. Desorption and regeneration studies are important to illustrate the properties of the adsorption process of Nd^{3+} onto the adsorbents. In this study, the adsorption−desorption cycle of Nd^{3+} ions was repeated three times to test the reusability of the adsorbents. A hydrochloric acid solution (pH = 1.0) was used as an eluent. The percentage desorption of Nd^{3+} from S_1 is shown in Table 7. The removal efficiency of the adsorbents decreased gradually, which was due to incomplete elution of the adsorbed metal on the adsorbents. After three cycles of use, the removal efficiency decreases to 86.7 %, and the evolution of the quantity of iron still stayed at 91 % in the microcapsules, the loss of iron being due to the dissolution of the magnetic nanoparticles in acid medium. Therefore, magnetic alginate P507 microcapsules remained magnetic enough to be extracted from the solution with a magnet. These experiments showed that the magnetic alginate P507 microcapsules could be reused several times without significant loss of initial properties.

CONCLUSIONS

In this study, magnetic alginate microcapsules containing extractant P507 were prepared for absorption and selective separation of neodymium from aqueous solutions. The prepared materials demonstrated very high adsorption capacity and selectivity for neodymium from the mixed Nd^{3+}/Co^{2+} and Nd^{3+}/Ni^{2+} solutions. The maximum uptake capacity of neodymium is 149.3 mg·g^{-1}. The adsorption process is dependent on several factors such as initial metal concentration, contact time, temperature, solution pH, and adsorbent dosage. The most optimum adsorbent dose is 0.05 g at pH 4.0 and 298 K. The adsorption data correlate well with the Langmuir isotherm model, while the kinetic data fit well the pseudosecond order model. On the basis of thermodynamic studies, it is showed that the adsorption process is spontaneous and endothermic with an activation energy of 20.75 kJ·mol^{-1}. The studies on FTIR spectra, adsorption isotherm, and pH suggest that solvent extraction and ion exchange are involved in neodymium adsorption onto the magnetic alginate P507 microcapsules and solvent extraction is prominent. The experiment of desorption and recycle indicates that the magnetic alginate P507 microcapsules can be used several times without significant loss of initial properties in the higher-temperature ranges.

AUTHOR INFORMATION

Corresponding Author

*Tel.: +86-021-65982287. Fax: +86-021-65982287. E-mail: wudongbei@tongji.edu.cn.

Funding Sources

The present work has been carried out under the financial support of "National Natural Science Foundation of China" (20706045).

REFERENCES

(1) Rao, T. R.; Biju, V. M. N. Trace determination of lanthanides in metallurgical environmental and geological samples. *Crit. Rev. Anal. Chem* **2000**, *30*, 179–184.

(2) Lee, M. S.; Lee, J. Y.; Kim, J. S.; Lee, G. S. Solvent extraction of neodymium ions from hydrochloric acid solution using PC88A and saponified PC88A. *Sep. Purif. Technol* **2005**, *46*, 72–78.

(3) Cox, M. Introduction to solvent extraction. In *Solvent Extraction Principles and Practice*; Rydberg, J., Cox, M., Musaikas, C., Choppin, G. R., Eds.; Marcel Dekker Inc.: New York, 2004; pp 11−15.

(4) Nishihama, S.; Sakaguchi, N.; Hirai, T.; Komasawa, I. Extraction and separation of rare earth metals using microcapsules containing bis(2-ethylhexyl)phosphinic acid. *Hydrometal* **2002**, *64*, 35–42.

(5) Mohammad, O.; Yuichi, N.; Hitoshi, M.; Ahmadi, S. J. Comparison of the batch and breakthrough properties of stable and plain alginate microcapsules with a chelating resin and an ion exchanger in Ag+ adsorption. *Ind. Eng. Chem. Res.* **2008**, *47*, 6742–6752.

(6) Mohammad, O.; Hitoshi, M.; Yuichi, N.; Kouichi, T. Equilibrium and kinetics of silver uptake by multinuclear alginate microcapsules comprising an ion exchanger matrix and Cyanex 302 organophosphinic acid extractant. *Ind. Eng. Chem. Res.* **2006**, *45*, 3633–3643.

(7) Pankhurst, Q. A.; Connoly, J.; Jones, S. K.; Dobson, J. Applications of magnetic nanoparticles in biomedicine. *J. Phys. D: Appl. Phys* **2003**, *36*, 167–181.

(8) Wu, D. B.; Zhao, J.; Zhang, L.; Wu, Q. S.; Yang, Y. H. Lanthanum adsorption using iron oxide loaded calcium alginate beads. *Hydrometal* **2010**, *101*, 76–83.

(9) Wu, D. B.; Zhang, L.; Wang, L.; Zhu, B. H.; Fan, L. Y. Adsorption of lanthanum by magnetic alginate-chitosan gel beads. *J. Chem. Technol. Biotechnol.* **2011**, *86*, 345–352.

(10) Donia, A. M.; Atia, A. A.; Elwakeel, K. Z. Selective separation of mercury (II) using magnetic chitosan resin modified with Schiff's base derived from thiourea and glutaraldehyde. *J. Hazard. Mater.* **2008**, *151*, 372–379.

(11) Ngomsik, A. F.; Bee, A.; Siaugue, J. M.; Cabuil, V.; Cote, G. Nickel adsorption by magnetic alginate microcapsules containing an extractant. *Water Res.* **2006**, *40*, 1848–1856.

(12) Ngomsik, A. F.; Bee, A.; Siaugue, J. M.; Talbot, D.; Cabuil, V.; Cote, G. Co (II) removal by magnetic alginate beads containing Cyanex 272. *J. Hazard. Mater* **2009**, *166*, 1043–1049.

(13) Xu, X. Q.; Shen, H.; Xu, J. R.; Xie, M. Q.; Li, X. J. The colloidal stability and core-shell structure of magnetite nanoparticles coated with alginate. *Appl. Surf. Sci.* **2006**, *253*, 2158–2164.

(14) Wu, R. J. Thermo analyses. In *The Application of Modern Analytic Technology in the Polymer*, the first edition; Shanghai Science Publishing Company: 1987; Chapter 9 (Chinese).

(15) Vijaya, Y.; Popuri, S. R.; Boddu, V. M.; Krishnaiah, A. Modified chitosan and calcium alginate biopolymer sorbents for removal of nickel (II) through adsorption. *Carbohydr. Polym.* **2008**, *72*, 261–271.

(16) Gotoh, T.; Matsushim, K.; Kikuchi, K. I. Preparation of alginate−chitosan hybrid gel beads and adsorption of divalent metal ions. *Chemosphere* **2004**, *55*, 135–140.

(17) Ngah, W. S. W.; Fatinathan, S. Adsorption of Cu (II) ions in aqueous solution using chitosan beads, chitosan-GLA beads and chitosan−alginate beads. *Chem. Eng. J.* **2008**, *143*, 62–72.

(18) Cao, J.; Liu, X. W.; Fu, R.; Tan, Z. Y. Magnetic P zeolites: Synthesis, characterization and the behavior in potassium extraction from seawater. *Sep. Purif. Technol.* **2008**, *63*, 92–100.

(19) Xiong, Y.; Adhikari, C. R.; Hidetaka, K.; Keisuke, O.; Katsutoshi, I.; Hiroyuki, H. Selective recovery of precious metals by persimmon waste chemically modified with dimethylamine. *Bioresour. Technol.* **2009**, *100*, 4083–4089.

(20) Guo, J. J.; Cai, J. B.; Su, Q. D. Ion imprinted polymer particles of neodymium: synthesis, characterization and selective recognition. *J. Rare Earths* **2009**, *27*, 22–27.

(21) Barros, C. F. F.; Sousa, F. W.; Cavalcante, R. M.; T Carvalho, V. F.; Dias, S.; Queiroz, D. C.; Vasconcellos, L. C. G.; Nascimento, R. F. Removal of Copper, Nickel and Zinc Ions from Aqueous Solution by Chitosan-8-Hydroxyquinoline Beads. *Clean* **2008**, *36* (3), 292–298.

(22) Chen, J. P.; Wang, L. Characterization of a Ca-alginate based ion-exchange resin and its application in lead, copper, and zinc removal. *Sep. Sci. Technol.* **2001**, *36*, 3617–3637.

(23) Jeon, C.; Nah, W.; Hwang, K. Y. Adsorption of heavy metals using magnetically modified alginic acid. *Hydrometallurgy* **2007**, *86*, 140–146.

(24) Park, J. S.; Han, C.; J Lee, Y. S.; Kim, D.; Kim, J. S.; Wee, J. H. Synthesis of extraction resin containing 2-ethylhexyl phosphonic acid. mono-2-ethylhexyl ester and its performance for separation of rare earths (Gd, Tb). *Sep. Purif. Technol.* **2005**, *43*, 111–116.